

Unzip instabilities: Straight to oscillatory transitions in the cutting of thin polymer sheets

P. M. REIS^{1(a)}, A. KUMAR², M. D. SHATTUCK² and B. ROMAN³

¹ *Department of Mathematics, Massachusetts Institute of Technology - Cambridge, MA 02139, USA*

² *Levich Institute, CCNY, CUNY - New York, NY 10031, USA*

³ *Physique et Mécanique des Milieux Hétérogènes (PMMH), UMR 7636 ESPCI/CNRS/Paris 6/Paris 7
10 rue Vauquelin, 75231 Paris CEDEX 05, France, EU*

received 21 December 2007; accepted in final form 23 April 2008

published online 5 June 2008

PACS 46.70.De – Beams, plates, and shells

PACS 62.20.M- – Structural failure of materials

PACS 62.20.F- – Deformation and plasticity

Abstract – We report an experimental investigation of the cutting of a thin brittle polymer sheet with a blunt tool. It was recently shown that the fracture path becomes oscillatory when the tool is much wider than the sheet thickness. Here we uncover two novel transitions from straight to oscillatory fracture by varying either the tilt angle of the tool or the speed of cutting, respectively. We denote these by *angle* and *speed unzip instabilities* and analyze them by quantifying both the dynamics of the crack tip and the final shapes of the fracture paths. Moreover, for the speed unzip instability, the straight crack lip obtained at low speeds exhibits out-of-plane buckling undulations (as opposed to being flat above the instability threshold) suggesting a transition from ductile to brittle fracture.

Copyright © EPLA, 2008

Over the past few years, the study of elasticity of thin sheets has been receiving increasing attention from the physics community [1]. During the deformation of a thin sheet, even if its material properties remain perfectly linear, large displacements can give rise to universal geometrical nonlinearities. These are responsible for a rich behavior which includes: stress focusing singularities [1], self-similar cascades [2–4] and wrinkling under tension [5]. The characteristic length scales of these phenomena have a non-trivial (fractional exponent) dependence on thickness, which is a signature of the singular limit of vanishing thickness. It is therefore not surprising that solving the full Foppl-von Kármán equations [6] for thin-sheet elasticity (which include the first non-linear terms) is in general a challenging endeavor. Thus, outside of applied engineering sciences, recent efforts have focused on developing novel tools by exploring relatively simple configurations, where the interplay between theory and experiments plays a crucial role. This approach becomes particularly relevant when considering situations where the elasticity of thin sheets couples to other phenomena such as fluid flow [7], surface tension [8],

ductile fracture [2] and adhesion [9], often leading to rich but highly non-trivial and counterintuitive problems.

In this spirit, the coupling of elasticity of thin sheets with fracture is a topic that has been receiving increasing attention over the past few years. Cutting and tearing of thin sheets has important practical application in a variety of contexts, including fracture in thin aeronautical structures [10], ship plating [11] in the naval industry, oscillatory fingering in colliding ice floes [12] and the development of resistant to wear but, at the same time, easy to tear polymer films for packaging. A generalized framework for coupling elasticity of thin sheets with fracture has, however, not yet been developed. Recent experiments [13,14] have introduced a novel configuration in which to study this coupling in a new perspective. In these experimental studies, it was shown that when a blunt cutting tool is forced through a thin brittle sheet, a strikingly regular wavy cut can be left behind, an example of which is presented in fig. 1f. Note that this is very different from other wavy crack paths that were observed in systems which do not involve the cutting by a blunt object (quasistatic propagation in thermal gradients [15,16], dynamic cracks under large bi-axial tension in rubber [17], and under pure mode-I loading

^(a)E-mail: preis@mit.edu

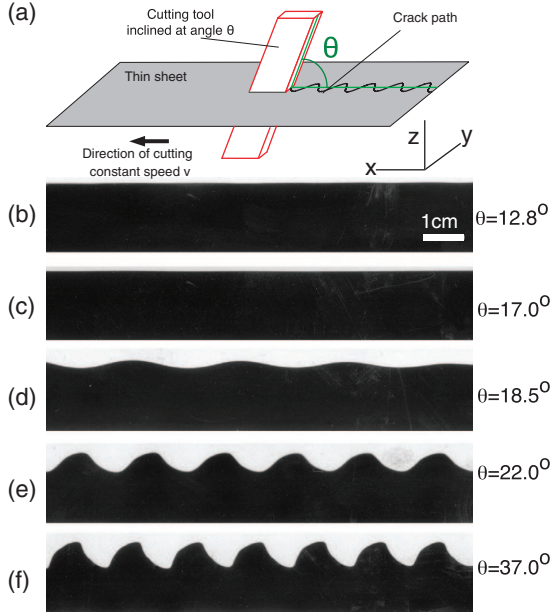


Fig. 1: (Color online) (a) Diagram of the experimental apparatus. (b-g) Series of scanned photographs of fracture patterns for various tilt angles (numerical value given at the right side of each image) for acetate sheet. The speed of the cutting tool was $v = 1.59$ mm/s. Cutting direction from is right to left.

when branching is inhibited [18]). Our oscillatory crack paths are non-sinusoidal, resembling a series of shark fins, and consist of smooth curves connected by sharp kinks which are associated with bursts of dynamic crack propagation. Both the amplitude, A , and wavelength, λ , of the crack pattern scale linearly with the width of the cutting tool, w . We showed [13] that when the width of the cutting tool and the thickness of the sheet, h , become comparable, the fracture is stabilized and becomes straight: we will refer to it as the *thickness unzip instability*. Far away from the width threshold, we have proposed a geometrical model for the mechanism underlying these oscillatory cracks [19,20]. The main ingredients of the model are the separation of the film's bending and stretching energies along with a fracture propagation rule based on Griffith's criterion [21]. In this way, the problem can be reduced to a geometrical construction which is sufficient to accurately reproduce the experimental fracture patterns using two physical parameters that relate to the material properties of the thin sheet. Both the non-linear shark fin shape of the cut and the dynamic burst are nicely predicted by this model. An alternative approach uses the criterion of maximal energy release rate [22]. For thin cutting tools (*i.e.* when the width is comparable to the sheet thickness), the bending and stretching energies over a typical distance w become comparable, the straight path is stabilized and our geometrical model breaks down.

Here we report experiments on two novel straight-to-oscillatory transitions uncovered by further exploring the parameter space of the system. We focus on two particular parameters: the tilt angle, θ , of the cutting tool with respect to the horizontal plane of the sheet (see fig. 1a) and the speed of cutting, v . In fig. 1(b-f) we present a series of crack paths for increasing tilt angles. Our previous work corresponds to the case of $\theta = 90^\circ$, where the cutting tool is perpendicular to the sheet. At high values of the tilt angle, of which fig. 1f is representative, the previously studied [13,14] nonlinear patterns reminiscent of shark fins are recovered. Here the crack paths consist of smooth arcs that are separated by kinks where there is a sharp change in the direction of propagation. By contrast, at low values of θ , an example of which is given in fig. 1b, the crack path is straight. In between these two limiting cases, a continuous straight-to-oscillatory transition occurs: smooth sinusoidal patterns emerge above a critical angle θ_c and become increasingly more nonlinear as θ is increased. We denote this transition by the *angle unzip instability*. Secondly, in the vicinity of this transition, an oscillatory path obtained by fixing θ above θ_c can be stabilized (*i.e.* becomes straight) if the cutting speed is reduced. We refer to this transition as the *speed unzip instability*. We proceed by performing a detailed quantitative analysis of the dynamics and shape of the fracture patterns for both of these instabilities. We note that the geometrical model [20] we have previously introduced for the case of $\theta = 90^\circ$ is unable to capture both of these novel transitions and that a theoretical description is still to be developed.

Experimental set-up. – A schematic diagram of our experimental apparatus is shown in fig. 1a. It consisted of a horizontal rectangular frame, dimensions (1.27×0.305) m², in which a flat thin polymer sheet was rigidly clamped along its two longest boundaries. With the aim of demonstrating that the phenomena we report are robust, we have used thin sheets of two different materials in our experiments: acetate (Grafix) and bi-oriented polypropylene (Innovia Films) with thicknesses $h_a = 127 \mu\text{m}$ and $h_p = 90 \mu\text{m}$, respectively. Both the acetate and polypropylene sheets were found to be isotropic such that identical results were obtained for experiments performed either along the machine or transverse directions. The cutting tool was an aluminum bar with rectangular cross-section (6.35×25.4) mm², with *cutting width* $w = 6.35$ mm, mounted onto a linear translational stage. The motion of the cutting tool could thereby be varied in the range $(10^{-4} < v < 10^{-1})$ ms⁻¹. Unless otherwise stated, the speed of the cutting tool was kept constant at $v = 1.59$ mms⁻¹. The tilt angle, θ , with respect to the horizontal sheet was measured to an accuracy of 0.1° using a tilt sensor (TrueTilt, The Fredericks Company) mounted directly on the cutting tool. For all experiments we fixed the widths of the frame, $D = 305$ mm, and of the cutting tool, $w = 6.35$ mm. We

have previously shown [13], for the case of $\theta = 90^\circ$, that the amplitude and wavelength of the fracture paths are independent of D and scale linearly with w .

From each experiment, we were interested in the dynamics of the crack tips during the cutting process as well as the shape of the final fracture paths. Hence, the data acquisition was twofold. Firstly, to study the dynamics a camera was mounted onto the translation stage which allowed for the region surrounding the crack tip to be imaged directly from above. The obtained digital videos could then be image-processed to extract the time series of the position of the crack tip, $[X'(t), Y'(t)]$, measured in the frame of reference of the cutting tool (*i.e.* $[X(t), Y(t)] = [X'(t) + vt, Y'(t)]$ in the lab frame) and the x - and y -axis directions are defined in fig. 1a. Secondly, to obtain the shape of the final fracture paths at a resolution significantly higher than that available from the digital videos, after each experiment one-half of the sheet containing the resulting crack was spray-painted black and digitized using an optical scanner at a resolution of 1200 dpi. This enabled the extraction of the $Y(X)$ shape of the crack lip to high precision using an edge detection technique.

Angle unzip instability. – We now quantify the transition from straight to oscillatory propagation, presented in the series of experimental photographs of fig. 1b,f, as θ is increased. For this purpose, we introduce the root mean square amplitude, A_{rms} , and the wavelength, λ , of the fracture patterns. The first is defined as $A_{rms} = \sqrt{\langle [Y(X)]^2 \rangle}$ and the latter is determined from the location of the main peak of the fast Fourier transform of $Y(X)$.

The dependence of A_{rms} on θ is plotted in fig. 2a for the acetate and the polypropylene sheets. Both materials show qualitatively identical results. At low values of θ , the crack paths are straight and $A_{rms} \sim 0$. The photograph in fig. 1b with $\theta = 12.8^\circ$ for the acetate sheet is representative of this regime. The film rides over the cutting tool, as it advances, up to a point where the opening stresses are large enough such that the sheet fractures symmetrically about the mid-point of the cutting tool. Above the tilt angle threshold, $\theta_c \sim 18^\circ$, the behavior of the cutting process is qualitatively different and the crack tip starts oscillating transversely about the mid-point of the cutting tool. The photographs of fig. 1c and d correspond to values of θ just before and after the transition, respectively. Past θ_c , the amplitude of the crack paths increases continuously, albeit sharply, with increasing angles, up to $\theta \approx 35^\circ$ where it levels-off. As one expects in a continuous bifurcation, close to threshold the pattern is sinusoidal, of which fig. 1d is an example. In fig. 2b we plot the wavelength of the fracture pattern, λ , as a function of θ . As the tilt angle is reduced from above towards θ_c , λ gradually increases in a divergence-like fashion. We stress the fact that similar results are obtained for both the acetate and polypropylene sheets suggesting that this results are robust for a range of materials. We highlight that this divergence-like increase of λ towards θ_c puts this angle

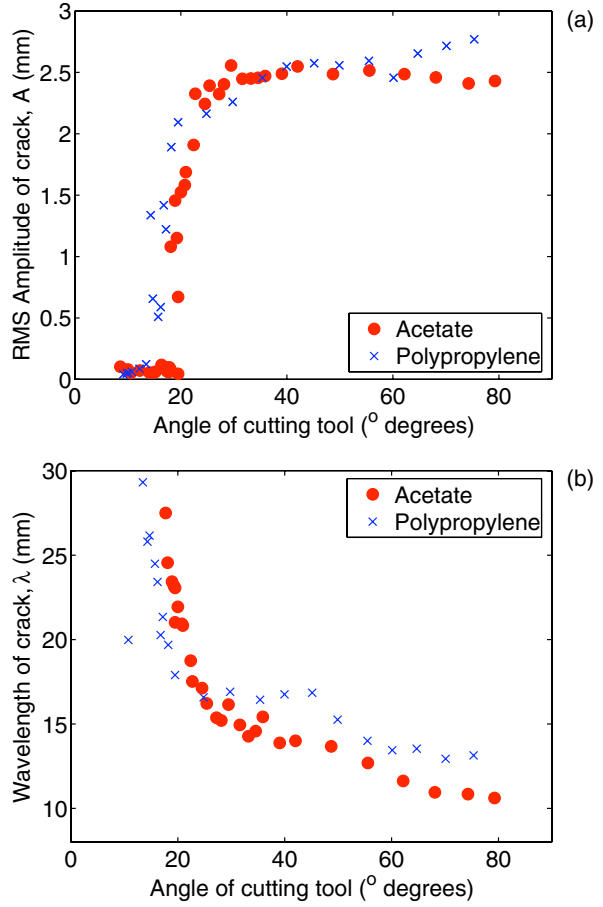


Fig. 2: (Color online) The dependence of the (a) root mean square amplitude, A_{rms} , and (b) the wavelength, λ , of fracture pattern on the tilt angle of the cutting tool for both, acetate (\bullet) and propylene (\times) sheets. Speed of cutting: $v = 1.59$ mm/s.

unzip instability in a different class of other oscillatory fracture scenarios, for example by thermal quenching of a glass strip [16], where at the transition point the wavelength assumes a finite value as the instability appears through a Hopf bifurcation [23]. Upon saturation, the shape of the cracks becomes highly nonlinear —fig. 1f— and the shark fin morphology typical of the $\theta = 90^\circ$ limiting case previously studied [13] is recovered. A possible explanation for the stabilization of the straight paths for small tilt angles is that as the film rides up the inclined tool, it is held on the boundaries of the tool, and tensile stresses develop into simple opening mode (mode-I loading), which may favor straight propagation.

We now turn to the dynamics of the angle unzip instability by examining the time-series of the $Y'(t)$ and $X'(t)$ coordinates of the crack tip, in the frame of reference of the cutting tool. In fig. 3 we present plots of $Y'(t)$ and $X'(t)$ for six representative values of θ . Prior to the critical tilt angle, θ_c , even though the crack lip is straight, the motion exhibits a highly periodic motion

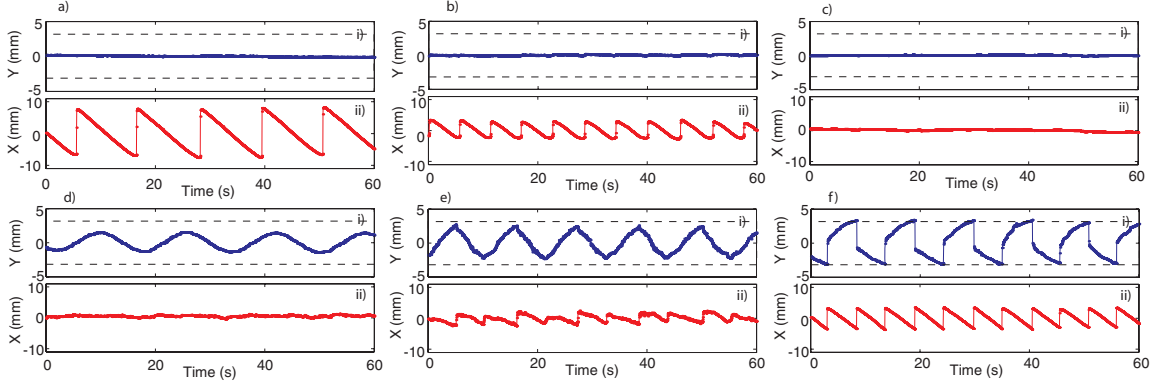


Fig. 3: (Color online) Time-series of i) $Y(t)$ and ii) $X(t)$ coordinates of the crack tip in the frame of reference of the cutting tool: a) $\theta = 12.8^\circ$ b) $\theta = 15.0^\circ$, c) $\theta = 17.0^\circ$, d) $\theta = 18.5^\circ$, e) $\theta = 22.0^\circ$, f) $\theta = 37.0^\circ$. Acetate sheet. The speed of the cutting tool was $v = 1.59$ mm/s moving along the x -direction while cutting the plastic sheet in the (x, y) -plane. The dashed lines represent the edge of the tool.

along the direction of cutting —figs. 3a,ii and b,ii for $\theta = 12.8^\circ$ and $\theta = 15.0^\circ$, respectively. As the cutting tool advances, the film rides up the tool, increasingly storing elastic energy up to a point when this becomes available to the crack tip, which then propagates dynamically. We observed crack velocities along the direction of cutting up to 0.3 ms^{-1} , (for the case shown in fig. 3a); which is two orders of magnitude faster than the tool’s speed. Shortly after the dynamic event, propagation ceases and the process is repeated periodically. The frequency/amplitude of this jagged motion along x increases/decreases with increasing θ . To test that this unsteady motion was not a result of the frictional interaction between the sheet and the cutting tool, we lubricated the region of contact near the tool but the jagged dynamics persisted. This suggests that it is a genuine effect related to the relaxation of elastic energy in the sheet. A possible explanation for this stick-slip propagation could be that the material toughness may decrease with crack speed in the regime considered (due to plastic dissipation favored at small speeds). Crack propagation from rest would then require a higher energy release rate, overshooting the crack toughness for a higher speed. This would lead to crack acceleration and thus to a dynamic jump.

Just before the oscillatory transition, the time-series of both coordinates of the crack tip are flat such that the fracture propagates straight at a speed equal to that of the cutting tool —fig. 3c for $\theta = 17.0^\circ$. Past the transition at θ_c , the crack tip starts to smoothly oscillate in the direction perpendicular to the cutting —fig. 3d. This oscillatory motion is sinusoidal with a peak-to-peak amplitude smaller than the width of the cutting tool (represented by the two horizontal dashed lines in fig. 3) and the fracture propagates smoothly along x , at the same speed as the cutting tool. Upon further increasing of the tilt angle, for example for $\theta = 22.0^\circ$ in fig. 3e, $Y'(t)$ becomes increasingly nonlinear with a more triangular shape and the bursts of dynamic propagation in $X'(t)$

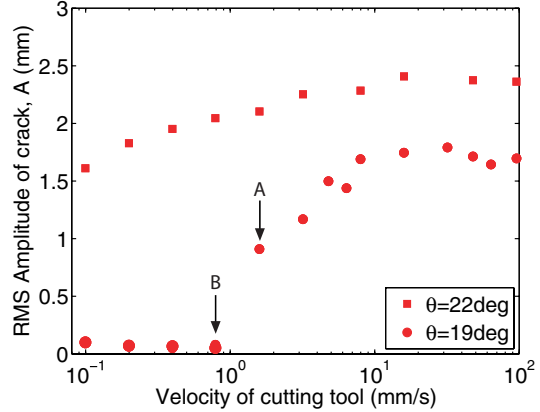


Fig. 4: (Color online) Dependence of the root mean square amplitude, A_{rms} , of fracture pattern on the speed of the the cutting tool for the acetate sheet plotted in log-linear scale. $\theta = 19.0^\circ$ (circles) and $\theta = 22.0^\circ$ (squares). Point A is located at $v = 1.59$ mm/s and point B at $v = 0.40$ mm/s.

reappear. Eventually, the amplitude of the oscillations in the transverse direction equals the width of the cutting tool. Beyond this point, we recover the dynamics typical of the perpendicular case, $\theta = 90^\circ$, that was previously studied [13,14,20]: each single period consists of two smooth curves separated by a kink in both $X'(t)$ and $Y'(t)$, at which there is a sharp change in the direction of curvature. Moreover, propagation is primarily quasi-static but is interrupted by periodic bursts of dynamic propagation immediately after each kink, as reported in [13,14].

Speed unzip instability. – Finally, we explore the effect of the speed of cutting, v , near the transition point of the angle unzip instability, while keeping the tilt angle constant. In fig. 4 we present the dependence of A_{rms} on v , for two values of the tilt angle near θ_c , for the case

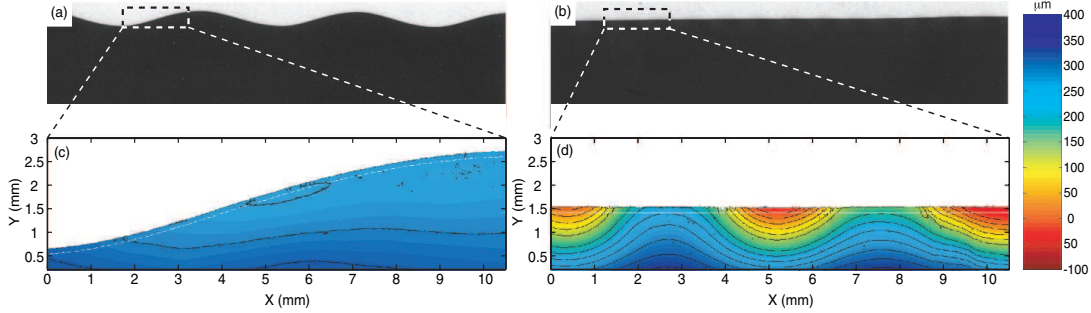


Fig. 5: (Color online) (a,b) Scanned photograph of the fracture pattern corresponding to the points a) A ($v = 1.59$ mm/s) and b) B ($v = 0.4$ mm/s) of fig. 4 (c,d). Height fields of a small region near crack lip for (a) and (b), respectively, obtained using the optical interferometric profiler. The color-map of the height is given by the color-bar on the right. The contour lines are separated by $25 \mu\text{m}$.

of using the acetate sheet. Since we varied the cutting speed over a wide range, ($10^{-4} < v < 10^{-1}$) ms^{-1} , and a significant dependence of the fracture process is only observed at low values of v , it is convenient to present the results in a logarithmic-linear axis. When the tilt angle is fixed at $\theta = 22.0^\circ$ (squares) the crack tip oscillate for all values of v . However, for $\theta = 19.0^\circ$ (circles), *i.e.* closer to θ_c , the behavior is qualitatively different. For high cutting speeds, $v \gtrsim 8 \text{ mms}^{-1}$, the crack paths are oscillatory with an approximately constant amplitude, $A_{rms} = (1.72 \pm 0.06)$ mm, whereas upon reducing the cutting tool speeds below $v \sim 8$ mm/s the amplitude of the fracture pattern decreases sharply towards zero. This suggests the existence of a new oscillatory-to-straight transition, for fixed angle of inclination, as the cutting speed is reduced below $v_c \sim 0.79$ mm/s. We denote this transition by the *speed unzip instability*.

To further explore the effect of the speed of the cutting tool on the morphology of the fractured sheets just above θ_c , we now focus on two representative points: A ($v = 1.59$ mm/s) and B ($v = 0.40$ mm/s) in fig. 4, immediately above and below the transition, respectively. The photographs of the top view for the fracture pattern for points A and B are shown in figs. 5a,b. As discussed in the previous paragraph, the crack path A is oscillatory (fig. 5a) and the crack path B is straight (fig. 5b). It is pertinent to look at the respective height profiles of the sheet in the region near the crack lip which are presented in figs. 5c,d. These were obtained using an optical interferometric profiler Microsurf 3D (Fogale Nanotech). The region neighboring the edge of the sheet produced by cutting at $v = 1.59 \text{ mms}^{-1}$ (point A) is approximately flat, or in other terms the fracture pattern is planar —fig. 5(c). This is what one would expect for brittle fracture. However, below v_c , the morphology of the sheet near the fractured edge is qualitatively different. Point B in fig. 5b,d is representative of this region where the crack path is straight but the height field of the sheet is increasingly undulated (out of plane) towards its edge (fig. 5d). For the case of point B , these undulations at

the edge have a wavelength of 5 mm and a peak-to-peak amplitude of $200 \mu\text{m}$. Note that the cracks obtained by cutting at $\theta = 22^\circ$ (squares in fig. 4), which were always oscillatory, did not exhibit any out-of-plane undulations throughout the whole range of v . Hence, the speed unzip instability occurs in the vicinity of the angle unzip instability, in a small region above $\theta > \theta_c$. It would be of interest, in future work, to perform a full mapping in the θ - v parameter space.

Surprisingly, similar out-of-plane buckling undulations have previously been observed in the experiments of Sharon *et al.* [2] where a thin plastic sheet is fractured in pure mode I, with a large degree of plastic deformation near the crack tip during the fracture process. The mismatch in the metric between the bulk of the sheet and the plastically deformed edge induces strong in-plane stresses such that the sheet minimizes its energy through buckling [24,25]. The resemblance between the out-of-plane undulation obtained below v_c in our system and the buckling cascade in the experiments of Eran *et al.* seem to suggest that a similar process may be at play. One possible explanation of this result is that at such low cutting tool speeds, the time-scale of the cutting process becomes comparable to the time-scale associated for the polymer (acetate) to flow and the material becomes ductile. Under this scenario, changing the speed of cutting reflects in varying the material properties of the polymer sheet with the possibility of entering a regime where oscillatory brittle fracture is no longer possible. It is worth mentioning that Gladden and Belmonte [26] have recently observed a transition from fluid flow past a cylinder to oscillatory solid-like tearing in a configuration similar to ours but using a viscoelastic fluid. All this suggests that one can regard the velocity unzip instability as an example of a brittle-to-ductile fracture transition.

Conclusion. — We have presented two new robust instabilities from straight to oscillatory crack path when a blunt object is driven through a brittle thin sheet: First, when the cutting tool is inclined under the *angle unzip*

instability threshold, the crack path is straight, even if the object is much larger than the thickness of the sheet. We suggest that this is due to the stretching (mode-I loading) obtained when the sheet climbs up the tool. An everyday analogy to this finding is the common knowledge that for cutting a thin sheet, an inclined knife yields a better control of the (straight) cutting than when holding the knife perpendicularly to the plane of the sheet. We showed that this bifurcation is continuous, but with a diverging wavelength near the threshold angle. Secondly, there is a threshold in the cutting speed below which the crack path becomes straight. We showed that this transition is also continuous, but that the stabilized straight paths exhibits out-of-plane buckling, suggesting that the fracture became ductile. This brittle-to-ductile transition may be due to time scales and plastic flow of the polymer but further investigation will be required to assert this. One may also question the role of plasticity in the *angle unzip instability*: as the sheet rides up the cutting tool, the singular behavior at the tip of the crack may be *blunted* by the contact of the thin sheet with the inclined tool. This effect is more prominent at low angles and may allow the system to enter into a ductile regime, therefore preventing the side-to-side oscillations. However no clear evidence of plastic flow were observed in that case, as the sheet remained flat.

Both of the angle and speed unzip instabilities are not captured by the previously developed theories [20,22]. We believe that these instabilities will stand as good test cases for theoretical models that couple elasticity of thin sheets and brittle fracture: they involve relatively simple configurations and present a set of clear and robust features. Another important point is that they are continuous (second order) bifurcations (contrary to the instability as a function of the width of the cutting), such that linear stability theories should be at reach, as in the case of thermal cracks [23]. We expect that our exploratory experimental study will motivate the development of new theoretical models and tools to help further understand the coupling of elasticity of thin sheets with fracture mechanics.

We thank S. DE VILLIERS for help with the preliminary experiments, A. PROVOST for allowing us to use his optical profilometer. We are grateful to B. AUDOLY and J. FINEBERG for helpful discussions and suggestions. MDS acknowledges funding from the National Science

Foundation and PMR and BR acknowledge funding from the European Union (MECHPLANT, NEST-Adventure).

REFERENCES

- [1] WITTEN T. A., *Rev. Mod. Phys.*, **79** (2007) 643.
- [2] SHARON E., ROMAN B., SHIN G. S., MARDER M. and SWINNEY H., *Nature*, **419** (2002) 419.
- [3] GIOIA G. and ORTIZ M., *Adv. Appl. Mech.*, **33** (1997) 119.
- [4] BENĀMAR M. and POMEAU Y., *Proc. R. Soc. London, Ser. A*, **453** (1997) 729.
- [5] CERDA E. and MAHADEVAN L., *Phys. Rev. Lett.*, **90** (2003) 074302.
- [6] LANDAU L. D. and LIFSHITZ E. M., *Theory of Elasticity* (Pergamon, New York) 1959.
- [7] SHELLEY M., VANDENBERGHE N. and ZHANG J., *Phys. Rev. Lett.*, **94** (2005) 094302.
- [8] BICO J., ROMAN B., MOULIN L. and BOUDADOUD A., *Nature*, **432** (2004) 690.
- [9] GILLE G. and RAU B., *Thin Solid Films*, **120** (1984) 109.
- [10] ATKINS A. G., *Endeavour*, **19** (1995) 2.
- [11] VAUGHAN H., *Nav. Archit.*, **97** (1978) 97.
- [12] VELLA D. and WETTLAUER J. S., *Phys. Rev. Lett.*, **98** (2007) 088303.
- [13] ROMAN B., REIS P. M., AUDOLY B., DE VILLIERS S., VIGUIÉ V. and VALLET D., *C. R. Mec.*, **331** (2003) 811.
- [14] GHATAK A. and MAHADEVAN L., *Phys. Rev. Lett.*, **91** (2003) 215507.
- [15] DEEGAN R., CHHEDA S., PATEL L., MARDER M., SWINNEY H., KIM J. and DE LOZANNE A., *Phys. Rev. E*, **67** (2003) 66209.
- [16] YUSE A. and SANO M., *Nature*, **362** (1993) 329.
- [17] DEEGAN R., PETERSAN P., MARDER M. and SWINNEY H., *Phys. Rev. Lett.*, **88** (2002) 14304.
- [18] LIVNE A., BEN-DAVID O. and FINEBERG J., *Phys. Rev. Lett.*, **98** (2007) 124301.
- [19] AUDOLY B., REIS P. M. and ROMAN B., *Phys. Rev. Lett.*, **94** (2005) 129601.
- [20] AUDOLY B., REIS P. M. and ROMAN B., *Phys. Rev. Lett.*, **95** (2005) 025502.
- [21] GRIFFITH A. A., *Phil. Trans. R. Soc. A*, **221** (1921) 163.
- [22] ATKINS A. G., *Eng. Fract. Mech.*, **74** (2007) 1018.
- [23] YANG B. and RAVI-CHANDAR K., *J. Mech. Phys. Solids*, **49** (2001) 91.
- [24] MARDER M., SHARON E., ROMAN B. and SMITH S., *Europhys. Lett.*, **62** (2003) 498.
- [25] AUDOLY B. and BOUDAUD A., *Phys. Rev. Lett.*, **91** (2003) 086105.
- [26] GLADDEN J. R. and BELMONTE A., *Phys. Rev. Lett.*, **98** (2007) 224501.